Carbonization of anthracene and phenanthrene. I. Kinetics and mesophase development

ARTICLE *in* ENERGY & FUELS · NOVEMBER 1993

Impact Factor: 2.79 · DOI: 10.1021/ef00042a049

4 AUTHORS, INCLUDING:

Robert G. Jenkins
University of Vermont
143 PUBLICATIONS **2,498** CITATIONS
SEE PROFILE

Semih Eser
Pennsylvania State University
124 PUBLICATIONS **1,261** CITATIONS
SEE PROFILE

Carbonization of Anthracene and Phenanthrene. 1. Kinetics and Mesophase Development

Teruhiko Sasaki,† Robert G. Jenkins,‡ Semih Eser,* and Harold H. Schobert

Fuel Science Program, Department of Materials Science and Engineering, The Pennsylvania State University, University Park, Pennsylvania 16802

Received May 17, 1993. Revised Manuscript Received August 17, 1993®

The investigation of the carbonization of anthracene and phenanthrene in microautoclave reactors has shown remarkable differences in the kinetics of formation of insoluble products and the extent of mesophase developed from these compounds. In previous work, single solvents were used to obtain kinetic data on the formation of insolubles. Three different solvents were used simultaneously in this study to monitor the formation of insolubles as a function of the solubility parameter of the solvent used. It is suggested that the differences in the extents of mesophase development from these compounds can be related to the kinetics for the formation of different solvent-insolubles, such as heptane- and toluene-insolubles during carbonization. The differences in carbonization reactivity of anthracene and phenanthrene and in mesophase development from these compounds have been explained using the concept of free valence index.

Introduction

The reactions of polycyclic aromatic hydrocarbons leading to the formation of solid carbonaceous materials are of importance both when the intent is to form a desired solid material, such as petroleum cokes, and when the formation of solids is undesirable, as in retrogressive reactions during coal or petroleum processing. Coal-derived liquids and heavy petroleum fractions are of sufficiently complex composition that their carbonization behavior is difficult to elucidate at a molecular level. Studies of the model compounds such as anthracene and phenanthrene can provide insights into the chemical behavior of the more complex materials. The formation of carbonaceous mesophase, an intermediate phase with a molecular alignment similar to that of nematic liquid crystals, is common to a remarkable variety of processes of practical interest, including carbonization of vitrinites of coking coals; the carbonization of heavy petroleum fractions, petroleum, and coal tar pitches, and the carbonization of thermoplastic polymers. The predominant molecular structures in the mesophase are highly condensed polycyclic aromatic hydrocarbons, which can form via the carbonization of simpler, smaller molecules such as anthracene and phenanthrene.

Prior studies on the carbonization of anthracene and phenanthrene have been reported.[1-9] Most of those studies pointed out significant differences in the carbonization behavior of these compounds. A common finding reported in the kinetic studies is the existence of an induction period prior to the appearance of the solvent insoluble products (e.g., pyridine insolubles) from both compounds.[9,10] Since anthracene is well-known to be more reactive than phenanthrene in many types of reactions,[11] the difference in behavior of these compounds suggests that we must take into account not only the steric differences imposed by the linear vs angular ring condensation but also fundamental differences in the carbonization reactivity and chemistry.

This paper presents the results on the kinetics of the early stages of anthracene and phenanthrene carbonization in relation to mesophase development. Recent previous work on these compounds[9,10] employed a single solvent for elucidating the kinetics of carbonization. In this study, three solvents with significantly different solubility parameters were used to follow the changes in the molecular size and complexity of the carbonization products. Results and discussion of the spectroscopic analysis of the products focused on the carbonization chemistry, and reaction mechanisms are presented in a companion paper.[12]

Experimental Section

The anthracene and phenanthrene were obtained in 98+% purity from Aldrich Chemical Co. and were used without further purification. The reactions were carried out in stainless steel microautoclave reactors of nominal 15-mL capacity. The reactors were pressurized to 5.0 MPa with nitrogen and were then immersed in a preheated sandbath using a Tecam Model IFB-51 industrial fluidized bath. The reactors were agitated during the reactions at

† Mitsubishi Oil Company Limited, 4-1, Ohigimachi, Kawasaki-Ku, Kawasaki, 210, Japan.

‡ University of Cincinnati, College of Engineering, Cincinnati, Ohio, 45221-0018.

• Abstract published in *Advance ACS Abstracts,* October 1, 1993.

(1) Wang, P. W.; Dachille, F. ; Walker, P. L., Jr. *High Temp.-High Pressures* **1974**, *6*, 127.
(2) Sharkey, A. G., Jr.; Shultz, J. L.; Friedel, R. A. *Carbon* **1966**, *4*, 355.
(3) Lewis, I. C. *Carbon* **1980**, *18*, 191.
(4) Walker, P. L., Jr. *Carbon* **1990**, *28*, 261.
(5) Walker, P. L., Jr.; Weinstein, A. *Carbon* **1967**, *5*, 13.
(6) Weintraub, A.; Walker, P. L., Jr. *Proceedings of the 3rd Conference on Industrial Carbons and Graphite*; Society of Chemical Industry: Letchworth, 1971, p 75.
(7) Evans, S.; Marsh, H. *Carbon* **1971**, *9*, 733.
(8) Evans, S.; Marsh, H. *Carbon* **1971**, *9*, 747.
(9) Peters, T. J.; Jenkins, R. G.; Scaroni, A. W.; Walker, P. L., Jr. *Carbon* **1991**, *29*, 981.
(10) Scaroni, A. W.; Jenkins, R. G.; Walker, P. L., Jr. *Carbon* **1991**, *29*, 969.
(11) Nishioka, M.; Lee, M. L. *Polynuclear Aromatic Compounds*; Ebert, L. B., Ed.; American Chemical Society: Washington, DC, 1988; Chapter 14.
(12) Sasaki, T.; Jenkins, R. G.; Eser, S.; Schobert, H. H. *Energy Fuels*, following paper in this issue.

0887-0624/93/2507-1039$04.00/0

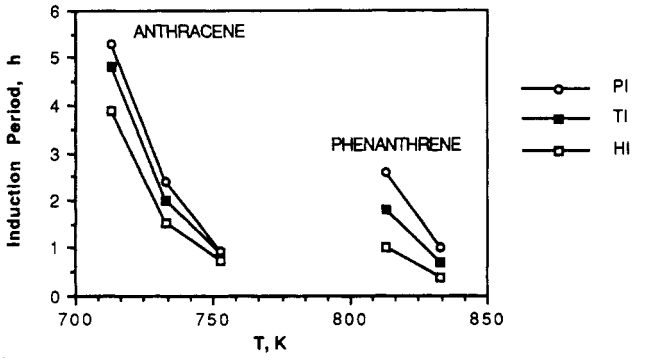

Figure 1. Induction periods for the formation of heptane-, toluene-, and pyridine-insolubles from anthracene and phenanthrene.

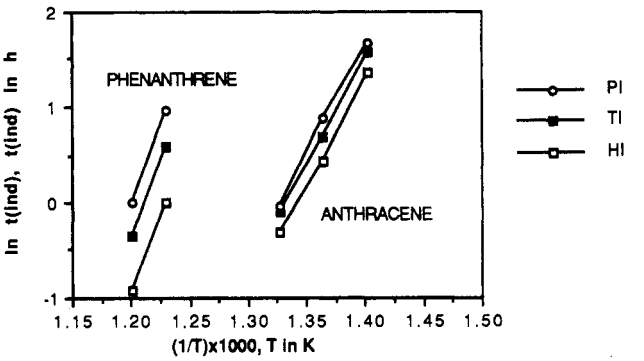

Figure 2. Arrhenius plots for the induction periods for the formation of heptane-, toluene-, and pyridine-insolubles from anthracene and phenanthrene.

a rate of 100 cycles/min with an amplitude of 2 cm. Carbonization of anthracene was carried out at 440, 460, and 480 °C for periods of 0.5–6.0 h. Phenanthrene was reacted at 540 and 560 °C for periods of 1.0–5.0 h. The initial sample size was 4.0 g in both cases.

At the end of a reaction, after decanting the liquids, the solid products were scraped from the reactors and weighed to determine the solid product yield. Samples of the solid products (0.5–0.8 g) were subjected to solvent extraction for 24 h in a nitrogen atmosphere using a Soxhlet apparatus. The solvents used were heptane, toluene, and pyridine, the solubility parameters of which are 7.5, 8.9, and 10.6 $(cal/cm)^{1/2}$, respectively.[13] The toluene was 99% purity grade; the other two were ACS certified reagent grade. All solvents were used without preliminary purification. The insoluble residues were dried for 24 h at 110°C at 13 kPa before weighing. The reproducibility of the solvent extractions reported as percentage of the insoluble products was within 1–3 wt % of the starting sample.

The mesophase development was followed by examining the polished sections of the solid products in polarized reflected light using a Model GFL Zeiss microscope equipped with polarizers and a $^1/_4$-wave gypsum retarder plate. Optical micrographs of the specimens were taken using a Zeiss camera (Model C-35) attached to the microscope.

Results and Discussion

Induction Periods. Different temperatures were employed for the carbonization of anthracene and phenanthrene because of the large difference in their reactivities. Only two different temperatures were used for phenanthrene carbonization, relying on the smooth change of carbonization rates with temperature observed for many compounds and feedstocks in this laboratory. The selected temperature ranges for each compound gave comparable induction periods for the appearance of the solvent insolubles and comparable overall rates for the nearly complete conversion into the insolubles. Figure 1 shows a plot of the induction periods preceding the appearance of heptane-, toluene-, and pyridine-insolubles versus the corresponding reaction temperatures of the two compounds. As expected, the induction periods increase with the increasing solubility parameter of the solvents used for extraction. In both cases, all the induction periods as well as the differences between the induction periods for different solvent-insolubles decrease sharply with the increasing temperature. The dependence of the induction periods on the solvent solubility parameters and the reaction temperature indicates a progressive increase in molecular size via initial reactions. The nature of these chemical processes is discussed in the companion paper.[12]

Table I. Apparent Activation Energies Calculated for the Chemical Changes Which Occur during the Induction Periods Prior to the Appearance of the Solvent-Insolubles

	E_i, kcal/mol	
solvent	anthracene	phenanthrene
heptane	45	62
toluene	45	63
pyridine	46	64

Assuming apparent first-order kinetics for the reactions taking place during the induction period, the induction times at different temperatures can be related to the global kinetic parameters for the appearance of solvent insolubles.[10] As explained in detail by Scaroni et al.,[10] a plot of the log of induction times ($\ln t_i$) against reciprocal temperature should give a straight line with a slope of E_i/R, where E_i is an apparent activation energy for the appearance of solvent solubles. The plots of $\ln t_i$ against $1/T$ for the formation of heptane-, toluene-, and pyridine-insolubles from anthracene and phenanthrene are shown in Figure 2. At least for the anthracene case, the data obtained at three temperatures were fitted well by straight lines. The apparent activation energies calculated for anthracene are given in Table I. It is interesting to note that the activation energies are almost the same (45 kcal/mol) for the appearance of the three solvent-insolubles, although the apparent induction periods associated with the different solvent-insolubles are quite different. The activation energies calculated for phenanthrene using the data obtained only at two different temperatures are also similar for the different solvent-insolubles (63 kcal/mol) and substantially higher than those for anthracene conversion. The reported activation energies for the appearance of pyridine insolubles calculated by the same method by Scaroni et al.[10] and Peters et al.[9] for anthracene and phenanthrene are 40 and 54 kcal/mol, respectively. The discrepancies between the activation energy values calculated in this study and those reported by others can be explained by the differences in the starting materials, experimental conditions, or data analysis.

It is worth emphasizing that despite the different induction periods observed for the appearance of different solvent-insolubles, similar apparent activation energies values were calculated for their initial formation from each compound. These findings suggest a progressive increase

(13) Mitchell, D. L.; Speight, J. G. *Fuel* **1973**, *52*, 149.

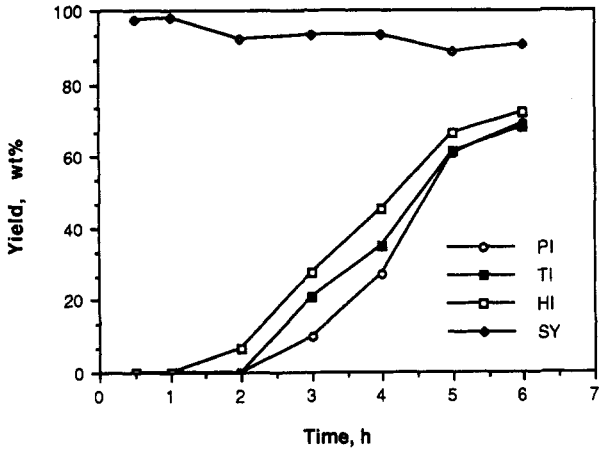

Figure 3. Yields of heptane-, toluene-, and pyridine-insolubles (HI, TI, and PI) and total solids (SY) from carbonization of anthracene at 480 °C.

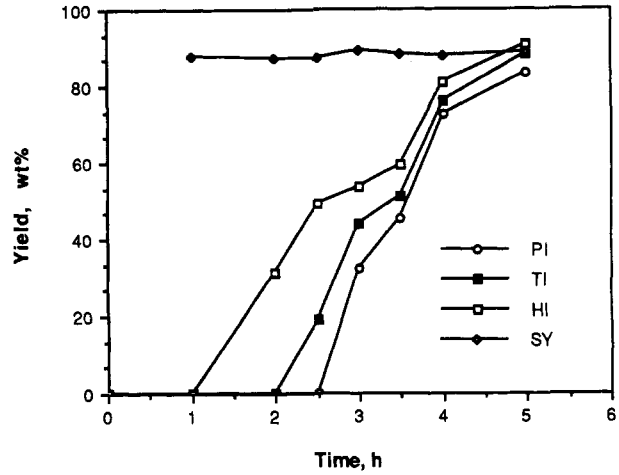

Figure 4. Yields of heptane-, toluene-, and pyridine-insolubles (HI, TI, and PI) and total solids (SY) from carbonization of phenanthrene at 540 °C.

in the molecular size of the early carbonization products which is governed by similar reaction mechanisms. The reactions of phenanthrene have, however, substantially higher activation energies than those of anthracene. This difference is explained below by the differences in the electronic configuration of these isomers.

Kinetics for the Formation of Solvent-Insolubles. Following the respective induction periods, solids start to form in the reactors. Typically, 96–98 wt % of the starting material was recovered in the liquid and solid products after carbonization, the balance being the gaseous products and the solids which could not be scraped from the reactor walls. The solid product yield,which ranged between 90 and 98%, was calculated from the mass of the solids scraped from the walls after decanting the liquid products. No wall effects were observed when the solid products were examined by polarized-light microscopy. The reproducibility of the yields of the solid products and solvent insolubles were typically within 2–3%. Figure 3 shows the solid product yield and the formation of heptane-, toluene-, and pyridine-insolubles from anthracene at 460 °C. The solid product yield decreases slightly, while the solid product becomes progressively more insoluble in the three solvents with the increasing reaction time. Curves of similar shape were obtained at 480 °C. The slight decrease in solid product yield with time is attributed to the formation of liquid and gaseous products. The curves for the three solvents are essentially parallel with different induction periods, suggesting that the kinetic parameters for the formation of different solvent-insolubles are essentially the same for the three solvents.

Figure 4 shows the yields of solid products and solvent-insolubles from phenanthrene carbonized at 540 °C. The lower reactivity of phenanthrene relative to anthracene is evident from the need to use significantly higher reaction temperatures to form comparable amounts of solvent-insolubles. Also, the solid product yields from phenanthrene are, in general, slightly lower than those from anthracene. Furthermore, different solvent-insolubles curves display different slopes for the three solvents, suggesting different kinetic parameters for each case. Similar behavior was observed at 560 °C with more pronounced differences in the slopes of the curves for the three solvents.

For kinetic analysis of the solvent-insolubles data, an apparent first-order kinetic behavior was considered for the formation of the insolubles with the assumption that the yield of gaseous products is negligible on a weight basis[9,10]

$$1 - \text{wt \% SI/wt \% SI}_{max} = \exp(-kt) \qquad (3)$$

where wt % SI represents the solvent-insolubles content of the carbonization products and and wt % SI_{max} represents the weight percent of starting anthracene or phenanthrene in the liquid phase at the reaction temperature, k is the rate constant, and t is the reaction time. The correction for the initial distribution of the starting compounds between liquid and gas phase is necessary because it is known that the vapor-phase pyrolysis of anthracene and phenanthrene is much slower than that in the liquid phase.[14,15] By use of the vapor–gas equilibrium calculations reported by Scaroni[10] and Peters,[9] it was found in this study that 92.0, 90.5, and 88.5 wt % of anthracene was initially in the liquid phase at temperatures 440, 460, and 480 °C and 94.9 and 94.6 wt % of phenanthrene was in the liquid phase at 540 and 560 °C, respectively

According to eq 3, a plot of $\ln(1 - \text{wt \% SI/wt \% SI}_{max})$ against time at constant temperature should give straight lines with slopes equal in absolute value to the corresponding rate constants. For both anthracene and phenanthrene, the insolubles data were fitted well by the apparent first-order kinetics model. As an example, the first-order plots for the formation of solvent-insolubles from anthracene at 480 °C are shown in Figure 5, indicating reasonably good fits of the data points by straight lines despite some scatter.

The apparent rate constants calculated for the solvent-insolubles from anthracene by the least-squares regression are given in Table II. The correlation coefficients of the least-squares regression are in the range 0.93–0.99 . The apparent activation energies and the preexponential factors calculated from the corresponding Arrhenius plots are also given in Table II. The calculated correlation coefficients are greater than 0.99 for the regression of all the Arrhenius plots used, providing confidence in the calculated values of the rate constants using linear

(14) Madison, J. J.; Roberts, M. M. *Ind. Eng. Chem.* **1958**, *50*, 237.
(15) Badger, G. M.; Donnelly, J. K.; Spotswood, T. M. *Aust. J. Chem.* **1964**, *17*, 138.

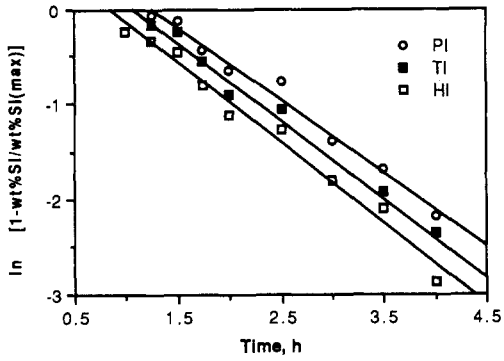

Figure 5. First-order plots for the formation of heptane-, toluene-, and pyridine-insolubles (HI, TI, and PI) from carbonization of anthracene at 480 °C.

Table II. Apparent Rate Constants Induction Periods and Arrhenius Parameters for the Formation of Heptane-, Toluene-, and Pyridine-Insolubles from Anthracene

solvent	T, °C	k, h^{-1}	t_{ind}, h	E, kcal/mol	A, h^{-1}
heptane	440	0.117	3.900	52	9.2×10^{14}
	460	0.344	1.530		
	480	0.805	0.735		
toluene	440	0.111	4.805	51	5.4×10^{14}
	460	0.300	2.000		
	480	0.740	0.900		
pyridine	440	0.096	5.300	52	6.4×10^{14}
	460	0.305	2.400		
	480	0.653	0.960		

regression. The standard deviation of the calculated activation energies is between 1 and 2 kcal/mol.

In parallel to the results obtained for the induction periods, the apparent activation energies for the formation of the three solvent-insolubles have very similar values, between 51 and 52 kcal/mol, with the apparent preexponential factors that range between 5.4×10^{14} and 9.2×10^{14} h^{-1}. These results are in agreement with values reported for the formation of pyridine-insolubles from anthracene.[10] The activation energy values were found to be approximately 6 kcal/mol higher than those calculated for the disappearance of anthracene during the induction periods. Scaroni et al.[10] also observed a 6 kcal/mol difference between the apparent activation energies calculated for the processes during and after the induction periods for the formation of pyridine insolubles. The authors suggested that the higher activation energy for the formation of pyridine insolubles could be attributed to the existence of an intermediate step between the disappearance of anthracene and the formation of pyridine insolubles. This reasoning is based on the assumption that the conversion level of anthracene at which the insolubles first appear is independent of temperature. The argument of an intermediate reaction step can be extended to the formation of toluene- and heptane-insolubles, as well, implying that the reaction intermediates involved are the common precursors to all three solvent-insolubles. The close similarities in the activation energies and preexponential factors calculated for the formation of the heptane-, toluene-, and pyridine-insolubles further suggest that the same reaction mechanisms are responsible for their formation following the respective induction periods. It is shown below that this is not the case for the carbonization of phenanthrene.

Table III shows the apparent rate constants, activation energies, and preexponential factors calculated for the formation of the solvent-insolubles from phenanthrene.

Table III. Apparent Rate Constants Induction Periods and Arrhenius Parameters for the Formation of Heptane-, Toluene-, and Pyridine-Insolubles from Phenanthrene

solvent	T, °C	k, h^{-1}	t_{ind}, h	E, kcal/mol	A, h^{-1}
heptane	540	0.758	1.050	53	1.7×10^{14}
	560	1.697	0.400		
toluene	540	0.690	1.860	61	1.4×10^{16}
	560	1.724	0.700		
pyridine	540	0.569	2.600	82	5.8×10^{21}
	560	1.959	1.000		

The correlation coefficients for the calculation of the rate constants ranged between 0.91 and 0.99. Since the solvent solubles data were collected only at two temperatures, no correlation coefficients are reported for the calculation of the activation energies and preexponential factors.

In contrast to the behavior of anthracene, the apparent activation energies for the formation of heptane- and pyridine-insolubles are significantly different from those calculated for the corresponding induction periods, while the values for toluene-insolubles are approximately the same in both cases. The significantly lower activation energy calculated for the formation of heptane-insolubles (53 kcal/mol) than that for the disappearance of phenanthrene during the induction period (62 kcal/mol) may suggest that the appearance of the heptane-insolubles catalyzes the further formation of these materials. In contrast, the activation energy for the formation of the pyridine insolubles (82 kcal/mol) is substantially higher than the corresponding activation energies calculated for the induction period processes. This observation, in turn, suggests that there are higher energy intermediate steps involved between the disappearance of phenanthrene and the formation of pyridine insolubles. Considering the differences in the activation energies for the initial appearance and subsequent formation of heptane- and pyridine-insoluble, one can infer that the similar activation energies calculated for both stages of toluene-insolubles result from a combination of an autocataytic effect with the presence of higher energy intermediate steps after the induction period.

Similar to the activation energies, the calculated preexponential factors for the formation of insolubles from phenanthrene vary over a wide range from 1.7×10^{14} h^{-1} for heptane insolubles to 5.8×10^{21} h^{-1} for pyridine insolubles. Peters et al.[9] reported an apparent activation energy of 75 kcal/mol for the formation of pyridine insolubles associated with an apparent preexponential factor of 3.5×10^{20} h^{-1}. Although there appears to be a compensation effect between the activation energy and preexponential factors calculated in this study and those reported by Peters et al.,[9] there is a large difference between the corresponding rate constants. However, the difference between the activation energies for the disappearance of phenanthrene and for the formation of pyridine insolubles is in good agreement with the 20 kcal/mol difference reported by Peters et al.[9] between the corresponding activation energies.

The large differences between the kinetic parameters for the disappearance of phenanthrene and the formation of insolubles imply that the appearance of the insoluble products is accompanied by significant changes in the energetics of the chemical reactions responsible for the formation of insolubles. This is in contrast to the smooth transition from the induction period reactions to the formation of the insolubles during the carbonization of anthracene. Further, the wide spread in the kinetic

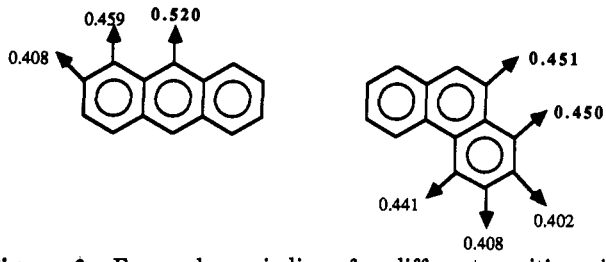

Figure 6. Free valence indices for different positions in anthracene and phenanthrene molecules.

parameters for the formation of different solvent insolubles suggests that, unlike in the case of anthracene, different reaction mechanisms are involved in the formation of the different solvent insolubles. These differences between the anthracene and phenanthrene carbonization are discussed in the accompanying paper in conjunction with the spectroscopic analyses of the carbonization products.[12] A notable feature of the kinetic data on phenanthrene carbonization is that at 560 °C both the rate constants for the formation of the solvent-insolubles and the corresponding induction periods increase in the order of increasing solubility parameters, i.e., heptane-, toluene-, and pyridine-insolubles. A possible explanation for this behavior is given below in terms of the relative reactivities of different sites on the phenanthrene molecule.

In contrast to the initial lower reactivity, during the respective induction periods, the formation of the solvent insolubles from phenanthrene is 2 to 3 times faster than the corresponding anthracene systems. A simple explanation for this reversal in comparative reactivity can be offered using the concept of free valence index. Free valence index, which can be determined by molecular orbital calculations,[16] represents a measure for the lack of bonding of an atom relative to its maximum bonding power. It was first suggested by Coulson[17] that free valence might be correlated with the ease with which free radicals react at a certain position in a molecule. Pullman,[18] Yokono et al.,[19] and others have used free valence to predict the chemical and thermal reactivity of aromatic hydrocarbons. The higher the free valence index of a site, the higher its reactivity toward free radicals. The free valence indices for anthracene and phenanthrene are shown in Figure 6.[20] For comparison, benzene has a free valence index of 0.398. The maximum free valence index of anthracene is at the 9 (or 10) position, and its value (0.520) is significantly higher than the next reactive site, the position 1 which has a free valence index of 0.459. This suggests that anthracene should be very reactive at the 9 and 10 positions. It has been proposed that polymerization occurs preferentially at the 9 and 10 positions.[1] The variation of indices for different ring positions in anthracene is 0.112 unit, the 2-position having the minimum value of 0.408. The large differences between the indices of different positions suggest that the reactions of anthracene will be selective regarding the ring position at which coupling occur. In contrast, not only are the free valence indices of phenanthrene substantially lower, suggesting a lower initial reactivity, but also the range between the highest and lowest value is only 0.049 unit, less than the difference between the indices of the first and second most reactive position in anthracene. This much smaller range suggests that once the resistance to reaction is overcome (i.e., the activation energy is surmounted by the use of higher temperatures), the subsequent reactions to form insolubles should proceed fast and be less selective regarding the sites at which reaction occurs. Thus, the higher activation energies calculated for the disappearance of phenanthrene during the induction periods, and subsequently higher rates of formation of the insolubles, can be attributed to the lower maximum free valence index of phenanthrene and the small differences between the indices of different sites compared to those of anthracene. The larger preexponential factors associated with larger activation energies for the formation of toluene- and pyridine-insolubles suggest that, indeed, once the activation energy barrier has been overcome, formation of these solvent-insolubles proceeds quickly. An exception to this argument is the kinetic parameters calculated for the formation of heptane-insolubles. The relatively low activation energy and small preexponential factor for the formation of heptane-insolubles can be attributed to the different nature of the dominating reactions that lead to the formation of heptane-insolubles, including autocatalysis.

Mesophase Development. Under the conditions employed, anthracene and phenanthrene gave rise to significantly different degrees of mesophase development. The optical textures of the semicokes obtained from both compounds at different temperatures are shown in Figure 7. Anthracene produced well-developed flow domains (200–500 μm) at 460 and 480 °C, while phenanthrene led to domains (20–30 μm) at 540 °C and mosaics (10 μm) at 560 °C. Some important factors for mesophase development are the ability and the rate of formation of large, planar molecules as well as the duration of the fluidity in the reaction medium.[21] Below, each factor is considered from a viewpoint of the relative reactivities of different sites in anthracene and phenanthrene molecules, as expressed by free valence indices.

In addition to the angular configuration of phenanthrene molecules which makes it difficult to form large planar structures without voids,[9] the planarity of the mesogens can be further impaired by oligomerization reactions, as discussed in the companion paper.[12] The differences in relative reactivities of ring positions in both compounds also offer an explanation for the lower degree of mesophase development from phenanthrene. In anthracene the high free valence index 9,10-positions are located diametrically across the molecule (Figure 6). As carbonization proceeds with coupling of the anthracene molecule, there will always be a position of a high free valence index available for further reaction. Continued condensation allows unimpeded growth of reasonably planar, discotic liquid crystal structures desirable for mesophase formation (see the accompanying paper[12] for a detailed discussion). In contrast, the high free valence positions in phenanthrene are on the same side of the molecule. Initial condensation of phenanthrene molecules can result in immediate consumption of both high free valence positions, interrupting the smooth growth of planar molecules, as perhaps

(16) Dewar, M. J. S. *The Molecular Orbital Theory of Organic Chemistry*; McGraw-Hill: New York, 1969.
(17) Coulson, C. A. *Faraday Soc. Discuss.* **1947**, *2*, 9.
(18) Pullman, B. *Proceedings, 3rd Conference on Carbon*; Pergamon Press: Oxford, 1960; p 3.
(19) Yokono, T.; Miyazawa, K.; Sanada, Y.; Marsh, H. *Fuel* **1979**, *58*, 692.
(20) Coulson, C. A.; Streitwieser, A., Jr. *Dictionary of π-Electron Calculations*; W. H. Freeman and Co.: San Francisco, CA, 1965.
(21) Marsh, H.; Walker, P. L., Jr *Chemistry and Physics of Carbon*; Walker, P. L., Jr., Thrower, P. A., Eds.; Marcel Dekker, Inc.: New York, 1979; Vol. 15, p 230.

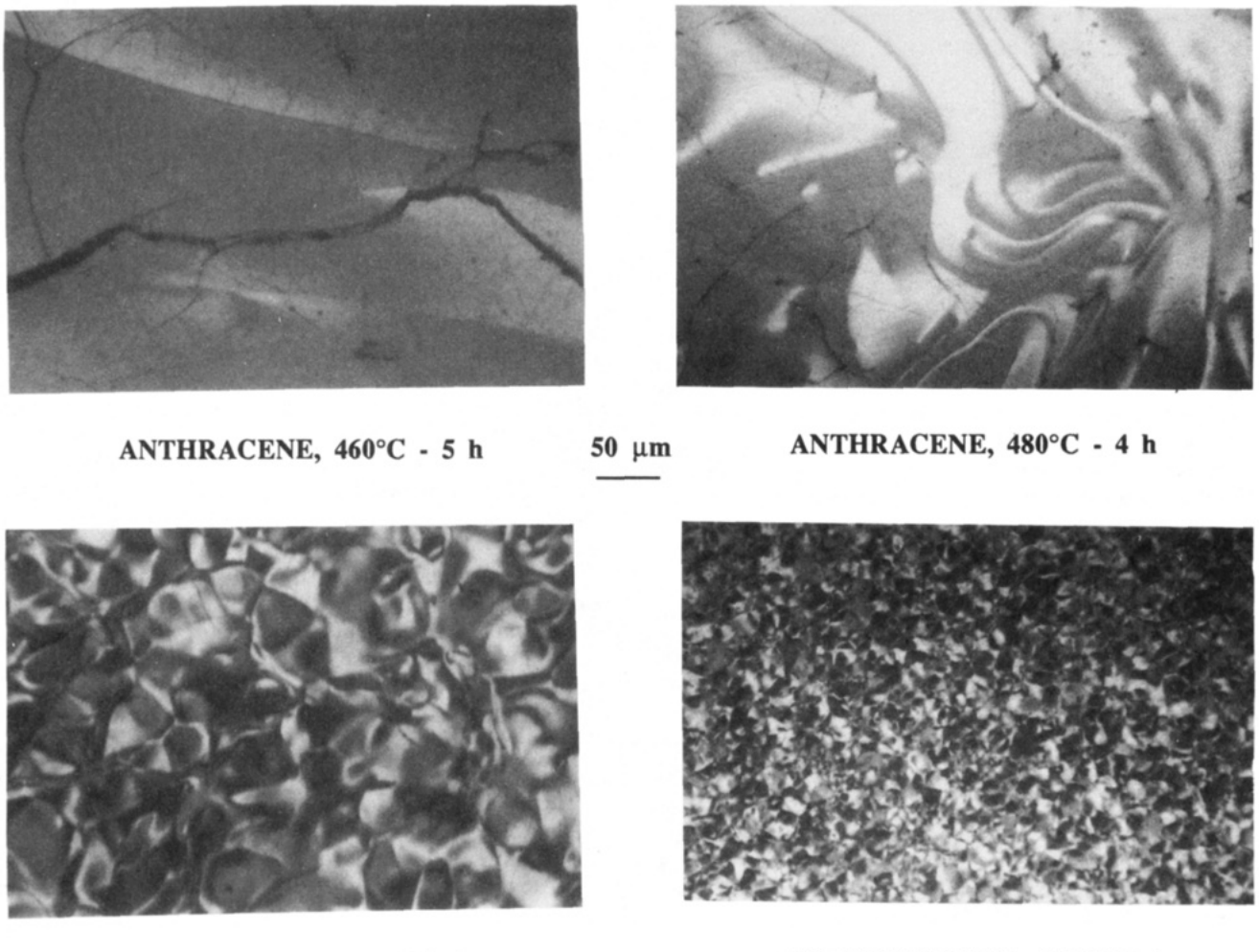

Figure 7. Polarized-light micrographs of the solids produced from anthracene and phenanthrene at different temperatures, showing the extent of mesophase development.

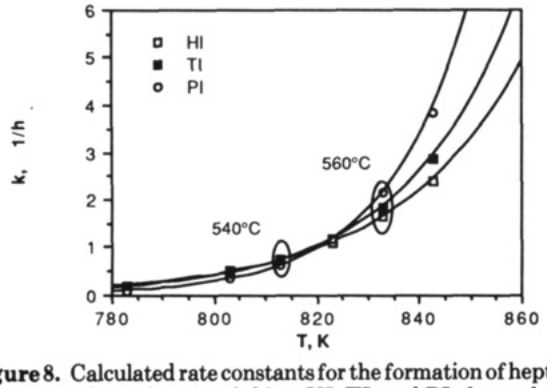

Figure 8. Calculated rate constants for the formation of heptane-, toluene-, and pyridine-insolubles (HI, TI, and PI) from phenanthrene.

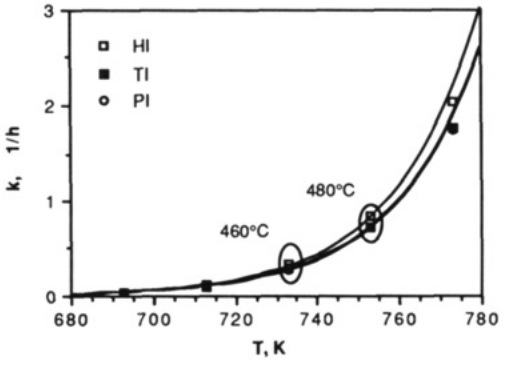

Figure 9. Calculated rate constants for the formation of heptane-, toluene-, and pyridine-insolubles (HI, TI, and PI) from anthracene.

reflected by the differences in the kinetic parameters for the formation of heptane-insolubles versus those of toluene- and pyridine-insolubles.

The mesophase development from both compounds appears to be hindered by the increasing temperatures of carbonization, as evident from the decreasing size of the extinction contours on the optical textures of the semicokes with the increasing temperature, as shown in Figure 7. It should be noted, however, that this effect was more pronounced in the case of phenanthrene where it resulted in the formation of mosaics at 560 °C, in agreement with the data reported by Peters et al.[9] The rapid formation of the large molecules would rapidly increase the viscosity of the reaction medium and, thus, hinder the diffusion and parallel orientation of these molecules. Figures 8 and 9 show the changes in the rate constants (calculated by using the apparent activation energies and preexponential factors obtained in this study) for the formation of insolubles from phenanthrene and anthracene, respectively, over extended temperature ranges. Figures 8 and 9 show that the rate constants for phenanthrene reactions increase much more than those for anthracene reactions upon a 20 °C temperature increase (i.e., from 460 to 480 °C for anthracene, from 540 to 560 °C for phenanthrene). As was mentioned before, a different feature in the

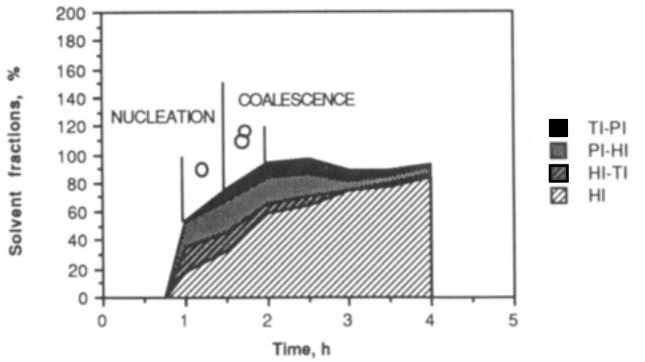

Figure 10. Relationships between the yields of different soventinsolubles and nucleation and coalescence stages of mesophase development during carbonization of anthracene at 480 °C.

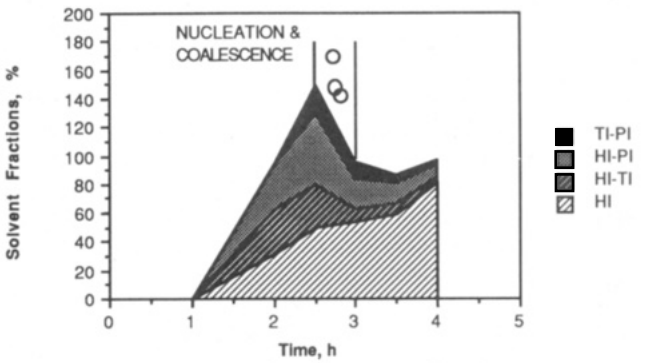

Figure 11. Relationships between the yields of different soventinsolubles and nucleation and coalescence stages of mesophase development during carbonization of phenanthrene at 540 °C.

phenanthrene plots is the crossover of the curves between 540 and 560 °C because of the higher activation energies for the formation of toluene- and pyridine-insolubles. In contrast, there is no crossover in the curves of the anthracene plots, indicating that the rate of formation of pyridine and toluene insolubles is always smaller than that of heptane insolubles. This represents, as was discussed before, a smooth, gradual increase in the size of the constituent molecules during carbonization, allowing long duration of fluidity for diffusion and orientation of the large molecules. As presented in the companion paper,[12] the prolonged fluidity of the anthracene products can be attributed, in part, to the extensive hydrogen transfer reactions. The more severe impairment of mesophase development from phenanthrene at the higher temperature employed can be explained by a much larger increase in the rate constants for the formation of toluene- and, especially, pyridine-insolubles.

In addition to the rate constants, another important and usually ignored parameter which affects the composition of the reaction mixtures, and thus the mesophase development, is the induction period associated with the appearance of the insoluble products. A good example of the significance of induction periods can be seen by comparing the carbonization products obtained from anthracene at 480 °C with those from phenanthrene at 540 °C. Tables II and III show that the rate constants calculated for the formation of different solvent insolubles (calculated at 480 °C for anthracene and at 540 °C for phenanthrene) are not very different from each other. However, the contents of the solvent-insolubles in the reaction products as a function of time are very different in the anthracene and phenanthrene products. This is shown in the area plots of Figures 10 and 11 where heptane-insolubles (HI) contents and the differences in solvent-insolubles contents (HI–TI), (HI–PI), and (TI–PI) are plotted versus time. Since differences between solvent-insolubles contents are added to the HI contents, these plots can have values greater than 100% in the ordinates as in Figure 11. The plots also mark, in the respective figures, the times for the appearance of mesophase spheres by a single circle and the inititation of the coalescence of spheres by two overlapping circles as observed by optical microscopy of the products. It can be seen in Figures 10 and 11 that, although the rate constants for the individual solvent-insolubles are comparable, the solvent-insolubles contents in anthracene and phenanthrene display different profiles. The large difference between pyridine-insolubles and heptane-insolubles (HI–PI) in the phenanthrene plot during the early stages of carbonization preceding the mesophase formation does not exist in the anthracene plot. The same trend is also seen for the difference between toluene-insolubles and heptane-insolubles (HI–TI). This disparity between the heptane-insolubles content and contents of toluene- and pyridine-insolubles is due to the relatively long induction periods for the appearance of pyridine- and toluene-insolubles from phenanthrene. As a result, the mesophase formation is delayed (no mesophase spheres is observed before 2.5 h of reaction time), while the heptane-insolubles content (and thus the overall viscosity) of the reaction mixture increases. The formation of mesophase spheres and their coalescence takes place concurrently with the rapid formation of toluene- and pyridine-insolubles, as indicated by the sharp drops in (HI–TI) and (HI–PI) values in Figure 11. The small mesophase spheres produced from phenanthrene appeared to have coalesced right after they were formed at 540 °C after 3 h. It is considered that the high viscosity of the reaction mixture and the large size of the molecular constituents did not allow much growth of the mesophase spheres before they coalesced. The optical texture of the solid product obtained from phenanthrene at 540 °C and 2.5 h, right before the formation of mesophase spheres, was totally isotropic. In contrast to phenanthrene, the nucleation and coalescence of mesophase spheres took place much earlier during the anthracene carbonization at 480 °C after 1 h and 1.75 h, respectively, and the two stages were distinctly separate as indicated in Figure 10, allowing the smooth growth of mesophase spheres before coalescence. The contents of the solvent insolubles when the mesophase spheres were first observed were 24.6% HI, 12.7% TI, and 5.5% PI for anthracene, compared to 53.5% HI, 44.1% TI, and 32.3% PI for phenanthrene. No mesophase spheres were observed in the pitch obtained from carbonization of phenanthrene at 540 °C for 2.5 h with insolubles contents of 50% HI, 19% TI, and 0% PI.

Clearly, all the kinetic parameters associated with the appearance and further formation of the solvent-insolubles (including the induction periods) are critically significant during the onset and development of mesophase. This observation suggests that the control over the kinetics of the carbonization processes can offer an effective means of controlling the mesophase development.

Conclusions

The carbonization of anthracene and phenanthrene shows very different kinetics for the appearance and subsequent formation of different solvent-insolubles. In contrast to a smooth transition from the kinetics involved

in the induction periods to the kinetics for the formation of solvent-insolubles from anthracene, phenanthrene carbonization is associated with abrupt changes in the kinetics of the chemical processes which take place during and after the induction periods. In addition, the kinetic parameters calculated for the formation of the three solvent-insolubles from anthracene are essentially the same, while those for the insolubles from phenanthrene are considerably different from each other. The lower initial reactivity of phenanthrene compared to anthracene as evident from the need to use higher temperatures to achieve comparable extents of conversion is contrasted with the higher reaction rate constants for the formation of insolubles after the respective induction periods have elapsed.

These differences in the kinetics of carbonization of anthracene and phenanthrene can be explained by the concept of free valence index. The comparison of the free valence indices of the two molecules provides an explanation for the initial low reactivity of phenanthrene as well as some of the differences observed in the kinetics of the formation of insoluble products and mesophase development from these compounds. It is generally agreed that mesophase formation derives from the production of lamellar molecules.[22] In anthracene the high free valence index 9,10-positions are located diametrically across the molecule. As carbonization proceeds with coupling of the anthracene molecule, there will always be a position of a high free valence index available for further reaction. Continued condensation allows unimpeded growth of reasonably planar, discotic liquid crystal structures desirable for mesophase formation, as discussed in the companion paper.[12] In contrast, the high free valence positions in phenanthrene are on the same side of the molecule. Initial condensation of phenanthrene molecules can result in immediate consumption of both high free valence positions. This geometric difference has three consequences. First, it is more difficult to form lamellar molecules during condensation of phenanthrene than of anthracene, and hence differences occur in mesophase development. Second, relatively bulky structures formed by phenanthrene condensation will have different hydrodynamic behavior in the melt than will the relatively planar structures from anthracene, resulting in higher viscosities of phenanthrene products which hinder mesophase development. Third, since positions of high free valence index are always available in anthracene condensation products, the successive condensation through heptane, toluene-, and pyridine-insolubles should occur with no significant change in activation energy, but since phenanthrene condensation can result in blockage of all available high free valence index positions, subsequent condensation would have to occur at positions of lower free valence index, with changes in activation energy. These arguments are based on differences in relative reactivities of different sites on the two molecules, geometric considerations, global kinetics of solvent-insolubles formation, and microscopic examination of solid products. These observations, must, however, derive from changes at the molecular level which can be followed by spectroscopic techniques. The spectroscopy and mechanisms of anthracene and phenanthrene carbonization are the subjects of a companion paper.[12]

Acknowledgment. The authors are grateful for the financial support for T. Sasaki and for supplies and analytical work provided by the Mitsubishi Oil Co. Ltd.

(22) Marsh, H.; Latham, C. S. *Petroleum Derived Carbons*; Bacha, J. D., Newman, J. W., White, J. L., Eds.; American Chemical Society: Washington, DC, 1986; Chapter 1.